Progress In Electromagnetics Research B, Vol. 31, 139–156, 2011

ANTENNA ARRAY BEAMFORMING IN THE PRESENCE OF SPATIAL INFORMATION UNCERTAINTIES

J.-H. Lee [1, *], G.-W. Jung [2], and W.-C. Tsai [2]

[1]Department of Electrical Engineering, Graduate Institute of Communication Engineering, and Graduate Institute of Biomedical Electronics and Bioinformatics, National Taiwan University, No. 1, Sec. 4, Roosevelt Rd., Taipei 10617, Taiwan

[2]Graduate Institute of Communication Engineering, National Taiwan University, No. 1, Sec. 4, Roosevelt Rd., Taipei 10617, Taiwan

Abstract—This paper deals with adaptive antenna array beamforming under spatial information uncertainties including steering angle mismatch, random perturbations in array sensor positions, and mutual coupling between antenna array sensors. To make antenna array beamformers robust against the spatial information uncertainties, we present an iterative method to obtain an appropriate estimate of the actual direction vector for each of the desired signals. The proposed method uses only the *a posteriori* information of the received array data. It invokes an appropriate objective function for estimation and solves the minimization of the objective function by using a gradient based algorithm. The convergence property of the proposed method is investigated. Simulation results are provided for showing the effectiveness of the proposed method.

1. INTRODUCTION

Adaptive antenna array beamforming for receiving signals has been widely considered due to many practical applications, such as sonar and radar signal processing [1–3] and wireless communications [4, 5]. An adaptive array beamformer can be viewed as a spatial filter designed for automatically preserving desired signals while canceling interference and noise [13, 14]. The weights of an antenna array beamformer are determined by adaptively processing the received signal data using

Received 30 March 2011, Accepted 7 June 2011, Scheduled 13 June 2011
* Corresponding author: Ju-Hong Lee (juhong@cc.ee.ntu.edu.tw).

spatial information. In practice, the spatial information may suffer from several uncertainties owing to steering angle mismatch, random perturbations in array sensor positions, and mutual coupling between array sensors. These three spatial uncertainties are referred to as the SRM uncertainties, where SRM is an abbreviation for the steering angle mismatch, random perturbations in array sensor positions, and mutual coupling between array sensors. Each of the SRM uncertainties results in a mismatch between the presumed and the actual direction vectors for the desired signals. The performance of an antenna array beamformer is significantly degraded by even a small mismatch [6].

To mitigate the effect of the spatial information uncertainties, several robust methods were recently developed by imposing either a spherical or an ellipsoidal uncertainty constraint directly on the steering vector for the conventional linearly main-beam constrained minimum variance (LCMV) beamforming [6–8]. These methods belong to the class of diagonal loading (DL) techniques which has been widely utilized to provide robustness against spatial uncertainty. It has been shown that this kind of ad hoc techniques usually helps to reduce the array beamforming sidelobes. They are robust against array steering vector errors if the diagonal loading factor is properly selected. However, the selection of the optimal diagonal loading factor is not clear. Moreover, it is somewhat difficult to find the relationship between the loading value and the level of uncertainty constraint or the preset level of robustness. A variable loading (VL) technique was presented by [9] to avoid the trade-off suffered by the DL techniques. Nevertheless, there are practically no papers dealing with the problem of adaptive broadband beamforming using two-dimensional (2-D) circular arrays under the combination of the SRM uncertainties in the literature.

In this paper, we present antenna array broadband beamforming using 2-D circular arrays with capabilities against the performance degradation due to the combination of the SRM uncertainties. We propose an iterative method to obtain an appropriate estimate of the actual direction vector for each of the desired signals. The proposed method invokes an appropriate objective function and solves the minimization of the objective function by using a gradient based algorithm. Simulation results show that the proposed method provides satisfactory broadband beamforming performance under the considered SRM uncertainties.

This paper is organized as follows. Section 2 formulates the problem of adaptive antenna array broadband beamforming using 2-D circular arrays in the presence of the SRM uncertainties. Then, a method is presented in Section 3 to provide robustness against the

considered problem. Section 4 shows several simulation examples for illustration and comparison. We conclude the paper in Section 5.

2. PROBLEM FORMLATION

Figure 1 shows that a 2-D uniform circular array (2-D UCA) consists of M antenna array sensors. There are $(J-1)$ adaptive tapped-delay coefficients or weights following each sensor. Let R be the radius and d be the spacing between two adjacent array sensors. Thus, we have $d = (2R)\sin(\pi/M)$. Assume that P uncorrelated broadband and far-field signals with complex waveforms $s_p(t)$ impinge on the 2-D array from direction angles (θ_p, ϕ_p), $p = 1, 2, \ldots, P$, off array broadside, where θ_p and ϕ_p represent the elevation and azimuth angles of the pth signal source, respectively. After converting the received signal into baseband, the data vector received by the 2-D UCA is expressed as follows:

$$\mathbf{x}(t) = \left[\mathbf{x}_1(t)^T \mathbf{x}_2(t)^T \ldots \mathbf{x}_j(t)^T \ldots \mathbf{x}_J(t)^T\right]^T \tag{1}$$

with size $MJ \times 1$, where the $M \times 1$ vector $\mathbf{x}_j(t)$ contains the received data of the $(j-1)$th delay section, $j = 1, 2, \ldots, J$. The superscript "T" denotes the transpose operation. The output of the 2-D UCA beamformer is given by $y(t) = \mathbf{w}^H \mathbf{x}(t)$, where $\mathbf{w}$ denotes the $MJ \times 1$ weight vector. The array response to a plane wave with frequency f and arrival angle (θ, ϕ) off array broadside is given by

$$r(f, \theta, \phi) = \mathbf{w}^H \{\mathbf{v}(f) \otimes \mathbf{a}(f, \theta, \phi)\}, \tag{2}$$

where $\mathbf{v}(f) = [1, e^{-j2\pi f\tau}, \ldots, e^{-j2\pi f(J-1)\tau}]^T$ with τ equal to the delay time between two adjacent nodes in the tapped-delay structure and $j = \sqrt{-1}$, $\mathbf{a}(f, \theta, \phi) = [e^{j2\pi f\psi_1(\theta,\phi)}, \ldots, e^{j2\pi f\psi_M(\theta,\phi)}]^T$ with $\psi_m(\theta, \phi) = R\{\cos(\phi - 2\pi(m-1)/M)\sin\theta\}/c$, $m = 1, 2, \ldots, M$, and $\otimes$ denotes the

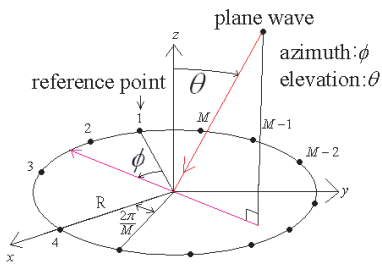

Figure 1. The geometric illustration of 2-D uniform circular array.

Kronecker product. Moreover, $\mathbf{a}(f,\theta,\phi)$ can be viewed as the ideal or presumed direction vector of a plane wave with frequency f and arrival angle (θ,ϕ) without spatial information uncertainties and tapped-delay operation. The vector $\mathbf{g}(f,\theta,\phi) = \mathbf{v}(f) \otimes \mathbf{a}(f,\theta,\phi)$ is referred to the array manifold vector associated with the direction angle (θ,ϕ). Then, we have that $\mathbf{A} = [\mathbf{v}(f) \otimes \mathbf{a}(f,\theta_1,\phi_1)\mathbf{v}(f) \otimes \mathbf{a}(f,\theta_2,\phi_2)\ldots\mathbf{v}(f) \otimes \mathbf{a}(f,\theta_P,\phi_P)]$ is the $MJ \times P$ source direction matrix. According to the linearly main-beam constrained minimum variance (LCMV) criterion, the broadband beamformer minimizes the power of the output signal $y(t)$ subject to some preset constraints. Assume that the first Q broadband signals are the desired signals. We formulate the broadband beamforming problem as follows:

$$\begin{array}{ll} \text{Minimize} & \mathbf{w}^H\mathbf{R}_{xx}\mathbf{w} \\ \text{Subject to} & \mathbf{A}_c^H\mathbf{w} = \mathbf{c}, \end{array} \tag{3}$$

where $\mathbf{R}_{xx} = E\{\mathbf{x}(t)\mathbf{x}(t)^H\}$ denotes the autocorrelation matrix of $\mathbf{x}(t)$, $\mathbf{A}_c = [\mathbf{v}(f) \otimes \mathbf{a}(f,\theta_1,\phi_1)\mathbf{v}(f) \otimes \mathbf{a}(f,\theta_2,\phi_2)\ldots\mathbf{v}(f) \otimes \mathbf{a}(f,\theta_Q,\phi_Q)]$ the $MJ \times Q$ constraint matrix for the frequency f in the desired frequency band, and $\mathbf{c} = [c_1 c_2 \ldots c_Q]^T$ the $Q \times 1$ gain vector. The optimal solution of (3) is given by

$$\mathbf{w} = \mathbf{R}_{xx}^{-1}\mathbf{A}_c\left(\mathbf{A}_c^H\mathbf{R}_{xx}^{-1}\mathbf{A}_c\right)^{-1}\mathbf{c}. \tag{4}$$

Let the spectral density of the input signal $s_p(t)$ be denoted by $S_p(f)$. It can be shown that the array spectral output due to $s_p(t)$ is given by $S_{yp}(f) = \mathbf{w}^H\mathbf{g}(f,\theta_p,\phi_p)S_p(f)\mathbf{g}(f,\theta_p,\phi_p)^H\mathbf{w}$. Hence, the array spectral output due to the Q desired signals $s_p(t)$, $p = 1,2,\ldots,Q$, is given by $S_{ys}(f) = \mathbf{w}^H(\mathbf{g}(f,\theta_1,\phi_1)S_1(f)\mathbf{g}(f,\theta_1,\phi_1)^H + \mathbf{g}(f,\theta_2,\phi_2)S_2(f)\mathbf{g}(f,\theta_2,\phi_2)^H + \ldots + \mathbf{g}(f,\theta_Q,\phi_Q)S_Q(f)\mathbf{g}(f,\theta_Q,\phi_Q)^H)\mathbf{w}$. Similarly, the array spectral output due to the P-Q interferers $s_p(t)$, $p = Q+1,\ldots,P$, is given by $S_{yi}(f) = \mathbf{w}^H(\mathbf{g}(f,\theta_{Q+1},\phi_{Q+1})S_{Q+1}(f)\mathbf{g}(f,\theta_{Q+1},\phi_{Q+1})^H + \mathbf{g}(f,\theta_{Q+2},\phi_{Q+2})S_{Q+2}(f)\mathbf{g}(f,\theta_{Q+2},\phi_{Q+2})^H + \ldots + \mathbf{g}(f,\theta_P,\phi_P)S_P(f)\mathbf{g}(f,\theta_P,\phi_P)^H)\mathbf{w}$. Moreover, the array spectral output due to the noise is given by $S_{yn}(f) = \mathbf{w}^H S_n(f)\mathbf{w}$, where $S_n(f)$ denotes the spectrum of the array input noise process. Accordingly, the array output signal-to-noise power ratio (SNR) and array output signal-to-interference plus noise power ratio (SINR) are computed by SNR $= P_{oS}/P_{oN}$ and SINR $= P_{oS}/(P_{oI} + P_{oN})$, where $P_{oS} = \sum_{k=1}^{K} S_{ys}(f_k)$, $P_{oI} = \sum_{k=1}^{K} S_{yi}(f_k)$, and $P_{oN} = \sum_{k=1}^{K} S_{yn}(f_k)$ due to the use of K-point discrete Fourier transform.

2.1. Steering Angle Mismatch

Under steering angle mismatch, a broadband beamformer will interpret the desired signals as interference and suppress them. Assume that the steering angle errors for the Q desired signals are $(\Delta\theta_q, \Delta\phi_q)$, $q = 1, \ldots, Q$. Without loss of generality, let the mth entry of the actual array response vector $\mathbf{a}_d(f, \theta_q, \phi_q)$ be expressed as $a_{dm}(f, \theta_q, \phi_q) = \exp(j\upsilon_{dqm})$. Similarly, let the mth entry of the presumed array response vector $\mathbf{a}(f, \theta_q, \phi_q)$ be expressed as $a_m(f, \theta_q, \phi_q) = \exp(j\upsilon_{qm})$. The mth entry of $\mathbf{a}(f, \theta_q, \phi_q)$ can further be expressed as $a_m(f, \theta_q, \phi_q) = \exp(j\upsilon_{dqm})\exp(-j\upsilon_{eqm})$, where υ_{eqm} is the phase angle deviation from the actual phase angle υ_{dqm}. By constructing an error vector $\mathbf{a}_e(f, \theta_q, \phi_q)$ with its mth entry defined as $a_{em}(f, \theta_q, \phi_q) = \exp(j\upsilon_{eqm})$, we can express the actual array response vector $\mathbf{a}_d(f, \theta_q, \phi_q) = \mathbf{a}(f, \theta_q, \phi_q) \odot \mathbf{a}_e(f, \theta_q, \phi_q)$, where $\odot$ denotes the Hadamard (or elementwise) product. To see the effect of steering angle mismatch on the array output, we consider the simplest case with $P = Q = 1$ and $c_1 = 1$ to obtain the output signal power

$$P_{oS} = E[|s_1(t)\mathbf{w}^H\{\mathbf{v}(f) \otimes (\mathbf{a}(f, \theta_1, \phi_1) \odot \mathbf{a}_e(f, \theta_1, \phi_1))\}|^2]. \tag{5}$$

Equation (5) shows that the steering angle mismatch attenuates the desired signal since

$$\begin{aligned} &|\mathbf{w}^H\{\mathbf{v}(f) \otimes (\mathbf{a}(f, \theta_1, \phi_1) \odot \mathbf{a}_e(f, \theta_1, \phi_1))\}| \\ &\quad < |\mathbf{w}^H\{\mathbf{v}(f) \otimes \mathbf{a}(f, \theta_1, \phi_1)\}| = 1. \end{aligned} \tag{6}$$

2.2. Random Perturbations in Array Sensor Positions

In the presence of random sensor position errors, we assume that $[x_m + \Delta x_m, y_m + \Delta y_m]$ is the actual location of the mth array sensor as shown in Figure 2. Δx_m and Δy_m denote the random sensor position errors. From Figure 2, we can see that the delay $\psi_m(\theta, \phi)$ of the signal with angle (θ, ϕ) at the mth array sensor becomes

$$\begin{aligned} \hat{\psi}(\theta, \phi) = {} & R\cos\left(\phi - \frac{2\pi(m-1)}{M}\right)\sin(\theta)/c \\ & +(\Delta x_m \cos(\phi) + \Delta y_m \sin(\phi))\sin(\theta)/c, \end{aligned} \tag{7}$$

where c denotes the speed of signal wave. Therefore, the actual $MJ \times P$ source direction matrix becomes $\hat{\mathbf{A}} = [\mathbf{v}(f) \otimes \hat{\mathbf{a}}(f, \theta_1, \phi_1)\mathbf{v}(f) \otimes \hat{\mathbf{a}}(f, \theta_2, \phi_2) \ldots \mathbf{v}(f) \otimes \hat{\mathbf{a}}(f, \theta_p, \phi_p)]$ with $\hat{\mathbf{a}}(f, \theta, \phi) = [e^{j2\pi f\hat{\psi}_1(\theta,\phi)}, \ldots, e^{j2\pi f\hat{\psi}_M(\theta,\phi)}]^T = \mathbf{a}(f, \theta, \phi) \odot \mathbf{\Theta}(f, \theta, \phi)$, where $\mathbf{\Theta}(f, \theta, \phi)$ is given by

$$\mathbf{\Theta}(f, \theta, \phi) = \left[e^{j2\pi f\varphi_1(\theta,\phi)}, \ldots, e^{j2\pi f\varphi_M(\theta,\phi)}\right]^T \tag{8}$$

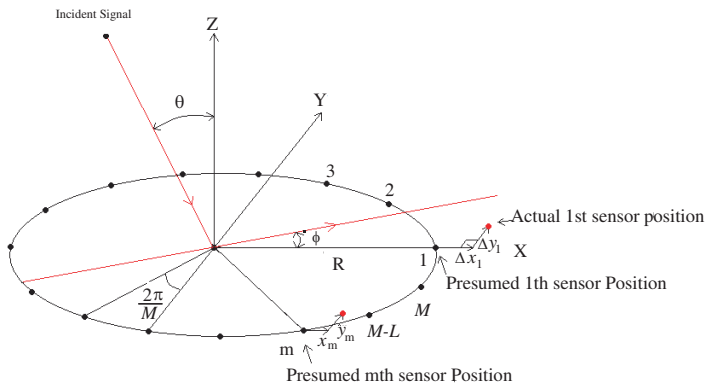

Figure 2. The geometric illustration of a UCA with sensor position errors.

with $\varphi_m(\theta, \phi) = (\Delta x_m \cos(\phi) + \Delta y_m \sin(\phi)) \sin(\theta)/c$. $\mathbf{\Theta}(f, \theta, \phi)$ represents the effect induced by the sensor position errors. Moreover, $\mathbf{\Theta}(f, \theta, \phi)$ depends on the source bearing (θ, ϕ) and $[\Delta x_m, \Delta y_m]$, $m = 1, 2, \ldots, M$. The existence of $\mathbf{\Theta}(f, \theta, \phi)$ introduces steering vector mismatch and array performance degradation.

2.3. Mutual Coupling

Consider the effect of the mutual coupling (MC) between antenna array sensors. We insert an MC matrix to the data model [10]. The $MJ \times P$ source direction matrix $\mathbf{A}$ is modified as follows: $\mathbf{A}_{MC} = [\mathbf{v}(f) \otimes \mathbf{a}_{MC}(f, \theta_1, \phi_1) \mathbf{v}(f) \otimes \mathbf{a}_{MC}(f, \theta_2, \phi_2) \ldots \mathbf{v}(f) \otimes \mathbf{a}_{MC}(f, \theta_p, \phi_p)]$ with $\mathbf{a}_{MC}(f, \theta_p, \phi_p)$ given by [10]

$$\mathbf{a}_{MC}(f, \theta_p, \phi_p) = \mathbf{C}\mathbf{a}(f, \theta_p, \phi_p), \tag{9}$$

where the MC matrix $\mathbf{C}$ of the 2-D UCA is created according to the fundamentals of electromagnetic theory as follows [11]:

$$\mathbf{C} = (Z_A + Z_T)(\mathbf{Z} + Z_T \mathbf{I}_M)^{-1}, \tag{10}$$

where Z_A is the sensor's impedance in isolation, Z_T is the impedance of the receiver at each sensor and is set to the complex conjugate of Z_A to achieve an impedance match for maximum power transfer, and $\mathbf{Z}$ is the mutual impedance matrix [11]. Equation (9) reveals that with the MCM taken into account, the actual direction vector of the pth signal with angle (θ_p, ϕ_p) and frequency f is given by $\mathbf{v}(f) \otimes \mathbf{a}_{MC}(f, \theta_p, \phi_p) = \mathbf{v}(f) \otimes \mathbf{C}\mathbf{a}(f, \theta_p, \phi_p)$ instead of $\mathbf{v}(f) \otimes \mathbf{a}(f, \theta_p, \phi_p)$. This significant

mismatch between $\mathbf{a}_{MC}(f, \theta_p, \phi_p)$ and $\mathbf{a}(f, \theta_p, \phi_p)$ deteriorates the performance of a 2-D UCA because $\mathbf{A}_c$ cannot provide the correct constraints on the desired signals which have the direction vectors $\mathbf{v}(f) \otimes \mathbf{a}_{MC}(f, \theta_p, \phi_p)$, $p = 1, 2, \ldots, P$.

3. PROPOSED METHOD

We present a method to find an appropriate estimate of the actual direction vector for each of the desired signals under the considered SRM uncertainties. Only the data vector $\mathbf{x}_1(t)$ received by the M array sensors without tapped-delay operation is required for estimation. The presumed delay for the signal with angle (θ, ϕ) at the mth array sensor is given by $\psi_m(\theta, \phi) = R\{\cos(\phi - 2\pi(m-1)/M)\sin\theta\}/c$, $m = 1, 2, \ldots, M$. The $M \times M$ correlation matrix $\mathbf{R}_{x1}$ of $\mathbf{x}_1(t)$ is given by

$$\mathbf{R}_{x1} = E\left\{\mathbf{x}_1(t)\mathbf{x}_1(t)^H\right\} = \sum_{i=1}^{M} \lambda_i \mathbf{e}_i \mathbf{e}_i^H, \tag{11}$$

where $\lambda_1 \geq \lambda_2 \geq \ldots \geq \lambda_D > \lambda_{D+1} = \ldots = \lambda_M = \sigma_n^2$ are the eigenvalues of $\mathbf{R}_{x1}$ in the descending order, $\mathbf{e}_i$ are the corresponding eigenvectors, and D is the dimensionality of the signal representation subspace. Ideally, the eigenvectors associated with the minimum eigenvalue σ_n^2 are orthogonal to the direction vectors of the signal sources. Hence, the subspaces spanned by $\mathbf{E}_n = \{\mathbf{e}_{D+1}, \ldots, \mathbf{e}_{MJ}\}$ (called the noise subspace) and $\mathbf{E}_s = \{\mathbf{e}_1, \mathbf{e}_2, \ldots, \mathbf{e}_D\}$ (called the signal representation subspace) are orthogonal. We can rewrite $\mathbf{R}_{x1}$ as follows:

$$\mathbf{R}_{x1} = \sum_{i=1}^{M} \lambda_i \mathbf{e}_i \mathbf{e}_i^H = \mathbf{E}_s \mathbf{\Lambda}_s \mathbf{E}_s^H + \mathbf{E}_n \mathbf{\Lambda}_n \mathbf{E}_n^H, \tag{12}$$

where $\mathbf{\Lambda}_s = \mathrm{diag}\{\lambda_1, \lambda_2, \ldots \lambda_D\}$ and $\mathbf{\Lambda}_n = \sigma_n^2 \mathbf{I}$, where $\mathbf{I}$ denotes the identity matrix with appropriate size. In the following, we present the estimation of the actual direction vector for each of the desired signals under the considered SRM uncertainties in the frequency domain. Taking the Fourier transform of $\mathbf{x}_1(t)$ yields an $M \times 1$ data vector in the frequency domain

$$\mathbf{X}_1(f) = \mathbf{A}_1(f)\mathbf{S}_s(f) + \mathbf{N}_1(f), \tag{13}$$

where the $M \times P$ matrix $\mathbf{A}_1(f) = [\mathbf{a}_1(f, \theta_1, \phi_1)\, \mathbf{a}_1(f, \theta_2, \phi_2) \ldots \mathbf{a}_1(f, \theta_P, \phi_P)]$. The pth column of $\mathbf{A}_1(f)$ is the actual direction vector associated with the M array sensors of the 2-D UCA without tapped-delay operation for the signal with angle (θ_p, ϕ_p). The $M \times 1$ vector $\mathbf{N}_1(f)$ is

the corresponding noise vector in the frequency domain. Assume that the noises with the same spectral densities are zero mean and uncorrelated with each other and the signals. An $M \times M$ spectral density matrix (SDM) associated with $\mathbf{X}_1(f)$ is given by

$$\mathbf{K}(f) = E\{\mathbf{X}_1(f)\mathbf{X}_1(f)^H\} = \mathbf{A}_1\mathbf{U}(f)\mathbf{A}_1^H + \sigma_n^2(f)\mathbf{I}_M, \tag{14}$$

where $\sigma_n^2(f)$ is the spectral density of the noises. $\mathbf{U}(f) = E\{\mathbf{S}_s(f)\mathbf{S}_s(f)^H\}$ is the signal SDM. For practical implementation, K_t data samples $x_{m,1}(k)$, $k = 1, 2, \ldots, K_t$, are taken by the mth array sensor, $m = 1, 2, \ldots, M$. We partition the K_t data samples into L overlapped subintervals $x_{m,1,\ell}(k)$, $\ell = 1, 2, \ldots, L$, with K samples for each and K_0 samples overlapped for adjacent subintervals. Let $X_{m,\ell}(f_k)$ be the K-point discrete Fourier transform (DFT) of $x_{m,1,\ell}(k)$. We construct vectors from $X_{m,\ell}(f_k)$ as follows:

$$\mathbf{X}_\ell(f_k) = [X_{1,\ell}(f_k)X_{2,\ell}(f_k)\ldots X_{M,\ell}(f_k)]^T. \tag{15}$$

A periodogram estimate of the $M \times M$ SDM at the frequency f_k is formed as follows:

$$\mathbf{K}_{x1}(f_k) = \frac{1}{L}\sum_{l=1}^{L}\mathbf{X}_\ell(f_k)\mathbf{X}_\ell(f_k)^H. \tag{16}$$

Similar to (12), we rewrite (16) as follows:

$$\begin{aligned}\mathbf{K}_{x1}(f_k) &= \sum_{i=1}^{M}\lambda_i(f_k)\mathbf{e}_i(f_k)\mathbf{e}_i(f_k)^H \\ &= \mathbf{E}_s(f_k)\mathbf{\Lambda}_s(f_k)\mathbf{E}_s(f_k)^H + \mathbf{E}_n(f_k)\mathbf{\Lambda}_n(f_k)\mathbf{E}_n(f_k)^H,\end{aligned} \tag{17}$$

where $\lambda_1(f_k) \geq \ldots \geq \lambda_D(f_k) > \lambda_{D+1}(f_k) = \ldots = \lambda_M(f_k) = \sigma_n^2(f_k)$ are the eigenvalues of $\mathbf{K}_{x1}(f_k)$ in the descending order and $\mathbf{e}_i(f_k)$ are the corresponding eigenvectors. Ideally, the eigenvectors associated with the minimum eigenvalue $\sigma_n^2(f_k)$ are orthogonal to the direction vectors of the signals. Therefore, the noise subspaces spanned by $\mathbf{E}_n(f_k) = \{\mathbf{e}_{D+1}(f_k), \ldots, \mathbf{e}_M(f_k)\}$ and the signal representation subspace spanned by $\mathbf{E}_s(f_k) = \{\mathbf{e}_1(f_k), \mathbf{e}_2(f_k), \ldots, \mathbf{e}_D(f_k)\}$ are orthogonal. Based on the above results, we propose an objective function for estimating the actual direction vectors as follows:

$$\begin{aligned}J(\mathbf{S}) &= \sum_{q=1}^{Q}(\mathbf{b}(f_k,\theta_q,\phi_q))^H\mathbf{E}_n(f_k)\mathbf{E}_n(f_k)^H(\mathbf{b}(f_k,\theta_q,\phi_q)) \\ &\quad -\kappa\exp\left\{-\sum_{q=1}^{Q}[(\mathbf{b}(f_k,\theta_q,\phi_q)-\mathbf{a}(f_k,\theta_q,\phi_q))^H(\mathbf{b}(f_k,\theta_q,\phi_q)\right. \\ &\quad \left.-\mathbf{a}(f_k,\theta_q,\phi_q))]/2\right\},\end{aligned} \tag{18}$$

where $\mathbf{b}(f_k, \theta_q, \phi_q)$ represents the estimate of the actual direction vector $\mathbf{a}_1(f_k, \theta_q, \phi_q)$ and the $MQ \times 1$ vector $\mathbf{S} = [\mathbf{b}(f_k, \theta_1, \phi_1)^T \mathbf{b}(f_k, \theta_2, \phi_2)^T \ldots \mathbf{b}(f_k, \theta_Q, \phi_Q)^T]^T$. $\mathbf{a}(f_k, \theta_q, \phi_q)$ represents the ideal or the presumed direction vector of a desired signal with frequency f_k and arrival angle (θ_q, ϕ_q) without spatial information uncertainties and tapped-delay operation. Each product $(\mathbf{b}(f_k, \theta_q, \phi_q))^H \mathbf{E}_n(f_k)\mathbf{E}_n(f_k)^H(\mathbf{b}(f_k, \theta_q, \phi_q))$ in the first term of (18) represents the squared norm of the projection of the estimated direction vector $\mathbf{b}(f_k, \theta_q, \phi_q)$ onto the noise subspace. The second term of (18) is related to the sum of the squared norms of the estimated direction error vectors. Minimizing the first term is equivalent to maximizing the orthogonality between the estimated direction vector $\mathbf{b}(f_k, \theta_q, \phi_q)$ and the noise subspace. The second term is utilized to prevent the estimated direction vector $\mathbf{b}(f_k, \theta_q, \phi_q)$ for the qth desired signal from becoming one of the direction vectors for the interferers. κ is a positive number providing the relative weight between the two terms. In general, a proper value of κ is determined by experiment. In the case of large angle separation between the desired signals and interferers, we prefer to set a small value for κ to enhance the orthogonality between the estimated direction vectors and the noise subspace. On the other hand, we may set a large value for κ to prevent the estimated direction vectors from becoming the interference direction vectors when the desired signals and interferers are close. We rewrite (18) as follows:

$$J(\mathbf{S}) = (\mathbf{S})^H \mathbf{W}(\mathbf{S}) - \kappa \exp\left\{-[(\mathbf{S} - \mathbf{S}_d)^H (\mathbf{S} - \mathbf{S}_d)]/2\right\}, \tag{19}$$

where the $MQ \times 1$ vector $\mathbf{S}_d = [\mathbf{a}(f_k, \theta_1, \phi_1)^T \mathbf{a}(f_k, \theta_2, \phi_2)^T \ldots \mathbf{a}(f_k, \theta_Q, \phi_Q)^T]^T$ contains the presumed or the ideal direction vectors $\mathbf{a}(f_k, \theta_q, \phi_q)$ without tapped-delay operation, $q = 1, 2, \ldots, Q$, and $\mathbf{W}$ is an $MQ \times MQ$ block diagonal matrix with the qth $M \times M$ diagonal block matrix given by $\mathbf{E}_n(f_k)\mathbf{E}_n(f_k)^H$, $q = 1, 2, \ldots, Q$. To find an appropriate estimate for each of the actual direction vectors, we minimize (19) by simply using a gradient-based algorithm. The gradient vector of $J(\mathbf{S})$ can be computed according to

$$\nabla_{\mathbf{S}} J(\mathbf{S}) = \mathbf{W}\mathbf{S} + (\kappa/2)\left[\exp\left\{-\left[(\mathbf{S}-\mathbf{S}_d)^H(\mathbf{S}-\mathbf{S}_d)\right]/2\right\}(\mathbf{S}-\mathbf{S}_d)\right]. \tag{20}$$

We then update $\mathbf{S}$ and the estimate $\tilde{\mathbf{a}}_1(f_k, \theta_q, \phi_q)$ of the actual direction vector $\mathbf{a}_1(f_k, \theta_q, \phi_q)$ as follows:

$$\begin{aligned} &\mathbf{S}^{(i+1)} = \mathbf{S}^{(i)} - \varepsilon \nabla_{\mathbf{S}} J(\mathbf{S}^{(i)}), \\ &\tilde{\mathbf{a}}_1(f_k, \theta_q, \phi_q)^{(i+1)} = \mathbf{b}(f_k, \theta_q, \phi_q)^{(i+1)}, \quad q = 1, 2, \ldots, Q, \end{aligned} \tag{21}$$

where the superscript i denotes the ith iteration and ε the preset positive step size. After obtaining $\tilde{\mathbf{a}}_1(f_k, \theta_q, \phi_q)$ for $k = 1, 2, \ldots, K$, we construct a new $MJ \times Q$ constraint matrix $\tilde{\mathbf{A}}_c$ by setting $\tilde{\mathbf{A}}_c =$

$[\mathbf{v}(f_k) \otimes \tilde{\mathbf{a}}_1(f_k, \theta_1, \phi_1)\mathbf{v}(f_k) \otimes \tilde{\mathbf{a}}_1(f_k, \theta_2, \phi_2) \ldots \mathbf{v}(f_k) \otimes \tilde{\mathbf{a}}_1(f_k, \theta_Q, \phi_Q)]$ for the frequency f_k in the desired frequency band. The optimal weight vector required by a tapped delay line is computed by $\mathbf{w} = \mathbf{R}_{xx}^{-1}\tilde{\mathbf{A}}_c(\tilde{\mathbf{A}}_c^H\mathbf{R}_{xx}^{-1}\tilde{\mathbf{A}}_c)^{-1}\mathbf{c}$. Then, the time-domain beamforming is performed by computing $y(t) = \mathbf{w}^H\mathbf{x}(t)$. Moreover, it would be expected that the resulting gradient approach for finding the optimal $\mathbf{S}$ can provide a more appropriate estimate of $\mathbf{S}$ since the resulting step size becomes variable due to the exponential term $\exp\{-[(\mathbf{S}-\mathbf{S}_d)^H(\mathbf{S}-\mathbf{S}_d)]/2\}$ as shown in (20). The convergence property of the proposed method is shown in the Appendix. Next, we present a simple scheme to effectively estimate the basis matrix $\mathbf{E}_n(f_k)$. First, we perform the eigenvalue decomposition on $\mathbf{K}_{x1}(f_k)$ of (16) to obtain the eigenvalues in the descending order. Then, the well-known MDL algorithm of [12] is employed to obtain the estimate $\hat{D}$ of the dimensionality D of the source representation space. Based on the estimate $\hat{D}$, we are able to construct the estimate of the basis matrix $\mathbf{E}_n(f_k)$ for computing the cost function of (18).

4. SIMULATION RESULTS

We use a 2-D UCA with the ratio of inter-element spacing d to the minimum wavelength λ of the desired signals equal to 0.5 for the simulation example. The simulation results are obtained by averaging 100 independent runs with independent noise samples for each run. The noise received by the 2-D UCA is spatially white with variance = 1. For the simulation example, our experience shows that the appropriate range for choosing κ is about $[0.00005, 0.00025]$ to effectively alleviate the effect of the considered SRM uncertainties on array performance. Accordingly, we adopt 0.0002 for κ to ensure that the estimated direction vectors are far away enough from the interference direction vectors. The ε used by the proposed method for simulations is set to 0.1. The iteration procedure is terminated when the norm of the gradient vector $\nabla_S J(\mathbf{S})$ is not greater than 0.01. We use a second-order autoregressive (AR) model for generating the desired broadband signals with power spectral density (PSD) $P_s(f)$ given by

$$P_s(f) = \frac{1}{\left|\left(1 - z_1 e^{-j2\pi f T_s}\right)\left(1 - z_2 e^{-j2\pi f T_s}\right)\right|^2}, \tag{22}$$

where T_s is the sampling period, $z_1 = 0.3\exp\{j2\pi f_L T_s\}$, $z_2 = 0.3\exp\{j2\pi f_H T_s\}$. The carrier frequency f_c of the AR broadband signals is set to 4 GHz. The fractional bandwidth B for the broadband signals is set to $B = (f_H - f_L)/f_c = 0.25$ with the low and high frequency edges equal to $f_L = 3.5$ GHz and $f_H = 4.5$ GHz

respectively. In contrast, we use another second-order model for creating the interferers by substituting $z_1 = 0.25\exp\{j2\pi f_L T_s\}$ and $z_2 = 0.25\exp\{j2\pi f_H T_s\}$ into (22). The sampling frequency $f_s = 1/T_s$ is set to $f_s = 4f_H$. The number of array data snapshots is $K_t = 1800$. The number of data snapshots for each subinterval $K = 10$ and $K_0 = 5$. The results of using the VL method of [9] are also shown for comparison.

Example: Here, we consider the case that four signal sources are impinging on the array with size $M = 9$ and number of tapped delays $(J-1) = 6$ from direction angles (θ, ϕ) equal to (75°, 40°), (15°, 300°), (35°, 265°), and (55°, 160°), respectively. Let the desired signals be the first two with $c_1 = c_2 = 1$ and the others be the interference. The sensor position errors Δx_m and Δy_m are independent Gaussian random variables with zero mean and the same variance σ_e^2. The MC matrix $\mathbf{C}$ of (10) is formed by setting $Z_A = 73 + j42.5$ (ohm) and $\mathbf{Z}$ is given by [11]

$$\mathbf{Z} = \begin{bmatrix} Z_A & Z_{12} & \cdots & Z_{1M} \\ Z_{21} & Z_A & \cdots & Z_{2M} \\ \vdots & \vdots & \ddots & \vdots \\ Z_{M1} & Z_{M2} & \cdots & Z_A \end{bmatrix}, \tag{23}$$

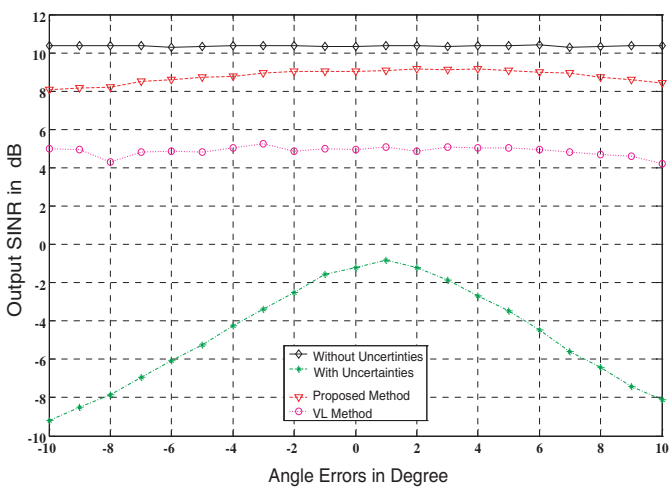

Figure 3. Array output SINR versus steering angle errors, where "uncertainties" means the SRM spatial information uncertainties.

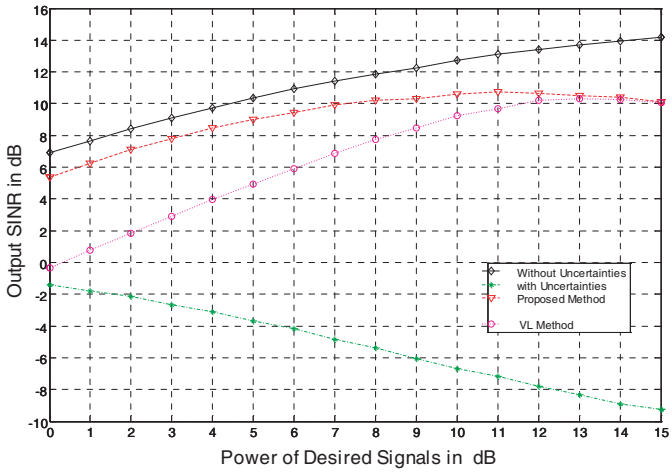

Figure 4. Array output SINR versus power of desired signals, where "uncertainties" means the SRM spatial information uncertainties.

where the entry Z_{mn}, $1 \leq m$, $n \leq M$, is given by [11]

$$Z_{mn} = \begin{cases} 30[0.5772 + \ln(2\xi\gamma) - C_i(2\xi\gamma)] \\ + j[30(S_i(2\xi\gamma))], & \text{for } m = n \\ 30[2C_i(\mu_0) - C_i(\mu_1) - C_i(\mu_2)] \\ - j[30(2S_i(\mu_0) - S_i(\mu_1) - S_i(\mu_2))], & \text{for } m \neq n \end{cases}, \tag{24}$$

where $\xi = 2\pi/\lambda$, $\gamma = \lambda/2$, $\mu_0 = \xi d$, $\mu_1 = \xi(\sqrt{d^2+\gamma^2}+\gamma)$, $\mu_2 = \xi(\sqrt{d^2+\gamma^2}-\gamma)$, λ is the signal wavelength, $C_i(\alpha) = \int_{\infty}^{\alpha}(\cos(x)/x)dx$ and $S_i(\alpha) = \int_0^{\alpha}(\sin(x)/x)dx$ are the cosine and sine integrals, respectively [11]. The initial guess of $\mathbf{b}(f_k, \theta_q, \phi_q)$ is set to the ideal or presumed direction vector $\mathbf{a}(f_k, \theta_q, \phi_q)$ for initiating the iterative procedure. Figure 3 depicts the simulation results including the output SINR versus the steering angle error with the sensor position error variance $\sigma_e^2 = 0.001\lambda^2$ under the SNRs of the four signals equal to 5, 5, 15, and 15 dB, respectively. We note that the proposed method provides significantly better robustness than the VL method over the range of $[-10°, 10°]$ for steering angle mismatch. Figure 4 plots the output SINR versus the power of the desired signals with $\sigma_e^2 = 0.001\lambda^2$, $(\Delta\theta_1, \Delta\phi_1) = (\Delta\theta_2, \Delta\phi_2) = (5°, 5°)$, and the interferers' power fixed at 15 dB. We note that the proposed method outperforms the VL method in dealing with the combination of the SRM uncertainties, especially in the case of the desired signals with low SNR. Figure 5 shows the output SINR versus σ_e^2 with $(\Delta\theta_1, \Delta\phi_1) = (\Delta\theta_2, \Delta\phi_2) = (5°, 5°)$ under the SNRs of the four signals equal to 5, 5, 15, and 15 dB,

respectively. This figure shows that the proposed method possesses almost consistent robust capability against random perturbations in array sensor positions for a range of $[0, 0.02]\lambda^2$ in error variance. Figure 6 presents the output SINR versus the number of data snapshots with $\sigma_e^2 = 0.001\lambda^2$ and $(\Delta\theta_1, \Delta\theta_2) = (5°, 5°)$ under the SNRs of the four signals equal to 5, 5, 15, and 15 dB, respectively. Although the VL method demonstrates better performance when the number of data snapshots is less than about 300, the proposed method can effectively cope with the performance degradation in the presence of the SRM uncertainties when sufficient data snapshots are available.

The logical reason why the proposed method can outperform the conventional VL method is that the proposed method finds an appropriate estimate of the actual direction vector for each of the desired broadband signals. By minimizing the proposed objective function shown by (18), the simulation results show that the obtained estimate $\tilde{\mathbf{a}}_1(f, \theta_q, \phi_q)$ is reasonably close to the actual direction vector $\mathbf{a}_d(f, \theta_q, \phi_q)$. In contrast, the VL method just alleviates the effect of the considered SRM spatial information uncertainties on antenna array beamforming by simply adding a loading factor into the data correlation matrix $\mathbf{R}_{xx}$. The loading factor is calculated to satisfy the constraint $\mathbf{w}^H\mathbf{R}_{xx}^{-1}\mathbf{w} = \delta$, where δ represents a robust level to be determined [9]. Nevertheless, the resulting alleviation is in general not sufficient to provide a satisfactory antenna array performance under the considered SRM spatial information uncertainties.

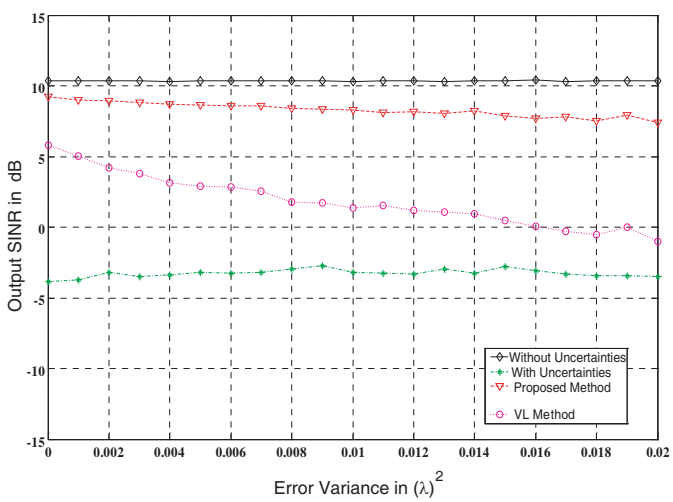

Figure 5. Array output SINR versus power of desired signals, where "uncertainties" means the SRM spatial information uncertainties.

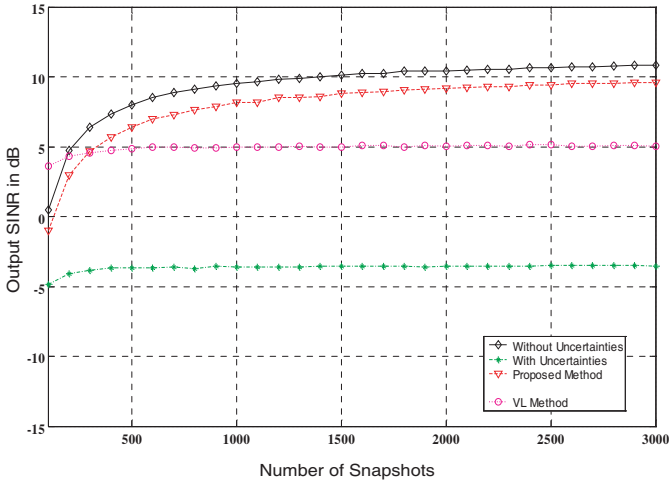

Figure 6. Array output SINR versus number of data snapshots, where "uncertainties" means the SRM spatial information uncertainties.

5. CONCLUSION

A novel method has been presented for antenna array broadband beamforming using 2-D circular antenna arrays under the spatial information uncertainties. We consider the spatial information uncertainties including the combination of steering angle mismatch, random array sensor position errors, and mutual coupling between antenna array sensors. The proposed method finds an appropriate estimate of the actual direction vector for each of the desired broadband signals. A theoretical proof for the convergence of the proposed method has been given. It has been confirmed by simulation results that the proposed method outperforms the existing diagonal loading technique under a variety of spatial information uncertainties.

ACKNOWLEDGMENT

This work was supported by the National Science Council of TAIWAN under Grant NSC97-2221-E002-174-MY3.

APPENDIX A.

To ensure the convergence of the proposed method, we show that the objective function of (18) possesses the property of $J(\mathbf{S}^{(i+1)}) <$

$J(\mathbf{S}^{(i)})$. For the sake of simplicity, we let the $MQ \times 1$ vector $\mathbf{B}^{(i)} = -\varepsilon \nabla_S J(\mathbf{S}^{(i)})$. Then, $(\mathbf{B}^{(i)})^H \mathbf{B}^{(i)} > 0$, i.e.,

$$\begin{aligned}&\left(\mathbf{B}^{(i)}\right)^H\Big\{-\varepsilon\Big[\mathbf{W}\left(\mathbf{S}^{(i)}\right)\Big]-(\varepsilon\kappa/2)\\&\Big[\exp\Big\{-\Big[\left(\mathbf{S}^{(i)}-\mathbf{S}_d\right)^H\left(\mathbf{S}^{(i)}-\mathbf{S}_d\right)\Big]/2\Big\}\left(\mathbf{S}^{(i)}-\mathbf{S}_d\right)\Big]\Big\}>0.\end{aligned} \tag{A1}$$

Hence,

$$\begin{aligned}&\left(\mathbf{B}^{(i)}\right)^H\Big[\mathbf{W}\left(\mathbf{S}^{(i)}\right)\Big]<-(\kappa/2)\\&\Big[\exp\Big\{-\Big[\left(\mathbf{S}^{(i)}-\mathbf{S}_d\right)^H\left(\mathbf{S}^{(i)}-\mathbf{S}_d\right)\Big]/2\Big\}\left(\mathbf{B}^{(i)}\right)^H\left(\mathbf{S}^{(i)}-\mathbf{S}_d\right)\Big]\\&\text{or } \mathrm{Re}\Big\{\left(\mathbf{B}^{(i)}\right)^H\Big[\mathbf{W}\left(\mathbf{S}^{(i)}\right)\Big]\Big\}<-(\kappa/2)\exp\Big\{-\Big[\left(\mathbf{S}^{(i)}-\mathbf{S}_d\right)^H\left(\mathbf{S}^{(i)}-\mathbf{S}_d\right)\Big]/2\Big\}\\&\times\mathrm{Re}\left\{\left(\mathbf{B}^{(i)}\right)^H\left(\mathbf{S}^{(i)}-\mathbf{S}_d\right)\right\},\end{aligned} \tag{A2}$$

where $\mathrm{Re}\{x\}$ represents the real part of x. From (21), we have the following approximation by neglecting the higher-order terms like $(\mathbf{B}^{(i)})^H(\mathbf{B}^{(i)})$

$$\begin{aligned}&\exp\left\{-\left[\left(\mathbf{S}^{(i+1)}-\mathbf{S}_d\right)^H\left(\mathbf{S}^{(i+1)}-\mathbf{S}_d\right)\right]/2\right\}\\&=\exp\left\{-\left[\left(\mathbf{S}^{(i)}+\mathbf{B}^{(i)}-\mathbf{S}_d\right)^H\left(\mathbf{S}^{(i)}+\mathbf{B}^{(i)}-\mathbf{S}_d\right)\right]/2\right\}\\&=\exp\Big\{-\Big[\left(\mathbf{S}^{(i)}-\mathbf{S}_d\right)^H\left(\mathbf{S}^{(i)}-\mathbf{S}_d\right)\Big]/2\Big\}\times\exp\Big\{-\Big[\left(\mathbf{S}^{(i)}-\mathbf{S}_d\right)^H\mathbf{B}^{(i)}\Big]/2\Big\}\\&\quad\times\exp\Big\{-\Big[\left(\mathbf{B}^{(i)}\right)^H\left(\mathbf{S}^{(i)}-\mathbf{S}_d\right)\Big]/2\Big\}\times\exp\Big\{-\Big[\left(\mathbf{B}^{(i)}\right)^H\left(\mathbf{B}^{(i)}\right)\Big]/2\Big\}\\&=\exp\Big\{-\Big[\left(\mathbf{S}^{(i)}-\mathbf{S}_d\right)^H\left(\mathbf{S}^{(i)}-\mathbf{S}_d\right)\Big]/2\Big\}\times\exp\Big\{-\Big[\left(\mathbf{B}^{(i)}\right)^H\left(\mathbf{B}^{(i)}\right)\Big]/2\Big\}\\&\quad\times\exp\left\{-\mathrm{Re}\left[\left(\mathbf{S}^{(i)}-\mathbf{S}_d\right)^H\mathbf{B}^{(i)}\right]\right\}\\&\approx\exp\Big\{-\Big[\left(\mathbf{S}^{(i)}-\mathbf{S}_d\right)^H\left(\mathbf{S}^{(i)}-\mathbf{S}_d\right)\Big]/2\Big\}\times\Big\{1-\mathrm{Re}\Big[\left(\mathbf{S}^{(i)}-\mathbf{S}_d\right)^H\mathbf{B}^{(i)}\Big]\Big\}.\end{aligned} \tag{A3}$$

It follows from (19) that

$$\begin{aligned}
J\left(\mathbf{S}^{(i+1)}\right) &= \left(\mathbf{S}^{(i+1)}\right)^H \mathbf{W}\left(\mathbf{S}^{(i+1)}\right) \\
&\quad -\kappa \exp\left\{-\left[\left(\mathbf{S}^{(i+1)}-\mathbf{S}_d\right)^H\left(\mathbf{S}^{(i+1)}-\mathbf{S}_d\right)\right]/2\right\} \\
&= \left(\mathbf{S}^{(i)}+\mathbf{B}^{(i)}\right)^H \mathbf{W}\left(\mathbf{S}^{(i)}+\mathbf{B}^{(i)}\right) - \kappa \exp \\
&\quad \left\{-\left[\left(\mathbf{S}^{(i)}+\mathbf{B}^{(i)}-\mathbf{S}_d\right)^H\left(\mathbf{S}^{(i)}+\mathbf{B}^{(i)}-\mathbf{S}_d\right)\right]/2\right\} \\
&\approx \left(\mathbf{S}^{(i)}\right)^H \mathbf{W}\left(\mathbf{S}^{(i)}\right) + \left(\mathbf{B}^{(i)}\right)^H \mathbf{W}\left(\mathbf{S}^{(i)}\right) \\
&\quad + \left(\mathbf{S}^{(i)}\right)^H \mathbf{W}\left(\mathbf{B}^{(i)}\right) + \left(\mathbf{B}^{(i)}\right)^H \mathbf{W}\left(\mathbf{B}^{(i)}\right) \\
&\quad -\kappa \exp\left\{-\left[\left(\mathbf{S}^{(i)}-\mathbf{S}_d\right)^H\left(\mathbf{S}^{(i)}-\mathbf{S}_d\right)\right]/2\right\} \\
&\quad \times\left\{1-\mathrm{Re}\left[\left(\mathbf{S}^{(i)}-\mathbf{S}_d\right)^H \mathbf{B}^{(i)}\right]\right\} \\
&\approx J\left(\mathbf{S}^{(i)}\right) + 2\mathrm{Re}\left[\left(\mathbf{S}^{(i)}\right)^H \mathbf{W}\left(\mathbf{B}^{(i)}\right)\right] + \mathrm{Re}\left[\left(\mathbf{S}^{(i)}-\mathbf{S}_d\right)^H \mathbf{B}^{(i)}\right] \\
&\quad \times\kappa\exp\left\{-\left[\left(\mathbf{S}^{(i)}-\mathbf{S}_d\right)^H\left(\mathbf{S}^{(i)}-\mathbf{S}_d\right)\right]/2\right\}. \qquad \text{(A4)}
\end{aligned}$$

Hence, we obtain from (A2) and (A4) that

$$\begin{aligned}
&J\left(\mathbf{S}^{(i+1)}\right) - J\left(\mathbf{S}^{(i)}\right) \\
&\approx 2\mathrm{Re}\left[\left(\mathbf{S}^{(i)}\right)^H \mathbf{W}\left(\mathbf{B}^{(i)}\right)\right] + \mathrm{Re}\left[\left(\mathbf{S}^{(i)}-\mathbf{S}_d\right)^H \mathbf{B}^{(i)}\right] \\
&\quad \times\kappa\exp\left\{-\left[\left(\mathbf{S}^{(i)}-\mathbf{S}_d\right)^H\left(\mathbf{S}^{(i)}-\mathbf{S}_d\right)\right]/2\right\} \\
&< 2\mathrm{Re}\left[\left(\mathbf{S}^{(i)}\right)^H \mathbf{W}\left(\mathbf{B}^{(i)}\right)\right] - 2\mathrm{Re}\left[\left(\mathbf{S}^{(i)}\right)^H \mathbf{W}\left(\mathbf{B}^{(i)}\right)\right] = 0. \qquad \text{(A5)}
\end{aligned}$$

The result shown by (A5) ensures the convergence under suitably small selections of ε.

REFERENCES

1. Musha, T. and T. Kumazawa, "Sonar signal processing based on the harmonic wavelet transform," *Proc. IEEE International*

Symposium on Underwater Technology, 291–295, Tokyo, Japan, April 2002.

2. Dekker, P. L., G. Farquharson, and S. J. Frasier, "Entropy based phase calibration of antenna arrays for digital beamforming remote sensing radars," *Proc. IEEE Radar Conference*, 445–452, Long Beach, California, USA, April 2002.
3. Younis, M., C. Fischer, and W. Wiesbeck, "Digital beamforming in SAR systems," *IEEE Trans. on Geoscience and Remote Sensing*, Vol. 41, No. 71, 1735–1739, July 2003.
4. Ramos, J., M. D. Zoltowski, and H. Liu, "Low-complexity space-time processor for DS-CDMA communications," *IEEE Trans. on Signal Processing*, Vol. 48, No. 1, 39–52, January 2000.
5. Zhang, Y., S. Weiss, and L. Hanzo, "Subband adaptive antenna array for wideband wireless communications," *Proc. the 3rd IEEE International Conference on Microwave and Millimeter Wave Technology*, 693–696, Beijing, China, August 2002.
6. Elnashar, A., S. M. Elnoubi, and H. A. El-Mikati, "Further study on robust adaptive beamforming with optimum diagonal loading," *IEEE Trans. on Antennas Propagat.*, Vol. 54, No. 12, 3647–3658, December 2006.
7. Wang, Z. and P. Stoica, "On robust Capon beamforming and diagonal loading," *IEEE Trans. on Signal Processing*, Vol. 51, No. 7, 1702–1715, July 2003.
8. Vincent, F. and O. Besson, "Steering vector errors and diagonal loading," *IEE Proc. — Radar, Sonar and Navigation*, Vol. 151, No. 6, 337–343, December 2004.
9. Gu, J. and P. J. Wolfe, "Robust adaptive beamforming using variable loading," *Proc. of The Fourth IEEE Workshop on Sensor Array and Multichannel Signal Processing*, 1–5, Waltham, MA, USA, July 12–14, 2006.
10. Huang, Z. and C. A. Balanis, "The MMSE algorithm and mutual coupling for adaptive arrays," *IEEE Trans. on Antennas Propagat.*, Vol. 56, No. 5, 1292–1296, May 2008.
11. Balanis, C. A., *Antennas Theory Analysis and Design*, Wiley, New York, 1997.
12. Wax, M. and T. Kailath, "Detection of signals by information theoretic criteria," *IEEE Trans. on Acoust., Speech, Signal Processing*, Vol. 33, No. 2, 387–392, April 1984.
13. Castaldi, G, V. Galdi, and G. Gerini, "Evaluation of a neural-network-based adaptive beamforming scheme with magnitude-only constraints," *Progress In Electromagnetics Research B*,

Vol. 11, 1–14, 2009.

14. Yang, P., F. Yang, Z. P. Nie, B. Li, and X. F. Tang, "Robust adaptive beamformer using interpolation technique for conformal antenna array," *Progress In Electromagnetics Research B*, Vol. 23, 215–228, 2010.